

Article

Numerical Simulation of Fire Suppression in Stilted Wooden Buildings with Fine Water Mist Based on FDS

Xinli Zhao , Shanyang Wei ^{*}, Yunyun Chu and Na Wang

School of Mining College, Guizhou University, Guiyang 550025, China

^{*} Correspondence: sywei1@gzu.edu.cn

Abstract: In this paper, to reflect a real fire combustion situation of stilted buildings with a typical wooden structure, we used FDS numerical simulation software to study the suppression effect of a fine-water-mist fire-extinguishing system under different working conditions. The influences of different mist droplet diameters, spray flows, and nozzle densities on the temperature change in the combustion area were analyzed and compared. The particle sizes of fog droplets exhibited a significant impact, indicating that the smaller the particle size, the faster the vaporization rate and the better the cooling effect. The cooling effect was better when the particle size was 150 μm or less when compared to the particle sizes of 200 and 300 μm . As the spray flow rate and nozzle density were increased, the fire field temperature decreased, and the cooling effect was enhanced, optimal at a water-mist flow rate of 8 L/min. Therefore, given the possible working conditions, the spray flow rate and the nozzle density should be high, while a suitable droplet size should be selected to achieve the best fire-extinguishing effect.

Keywords: FDS; water mist; fire; numerical simulation; wooden structure stilted buildings



Citation: Zhao, X.; Wei, S.; Chu, Y.; Wang, N. Numerical Simulation of Fire Suppression in Stilted Wooden Buildings with Fine Water Mist Based on FDS. *Buildings* **2023**, *13*, 207. <https://doi.org/10.3390/buildings13010207>

Academic Editors: Gang Zhang and Christopher Yu-Hang Chao

Received: 11 December 2022

Revised: 28 December 2022

Accepted: 10 January 2023

Published: 12 January 2023



Copyright: © 2023 by the authors. Licensee MDPI, Basel, Switzerland. This article is an open access article distributed under the terms and conditions of the Creative Commons Attribution (CC BY) license (<https://creativecommons.org/licenses/by/4.0/>).

1. Introduction

The long history of Chinese traditional wooden structures makes them valuable for architectural and cultural heritage, and the research on fire prevention and the protection of wooden structures and ancient buildings is an important part of architectural fire theory in order to ensure the continuation of China's traditional culture. According to statistics, in 2021, 788,000 fire reports were received by the national fire department, in which 1987 persons died and 2225 were injured, with direct property losses of CNY 6.75 billion. Moreover, housing fire accidents accounted for 34.5% of all accidents and 73.8% of all reported deaths [1]. Most of the stilted wooden buildings in southwest China form a series of continuous living units, and there are clusters of villages in which ethnic minority communities reside. The number of consumables or load-bearing components is small, and the spatial distribution is denser, providing favorable conditions for combustion. Moreover, the spacing between buildings is relatively small. Once a fire breaks out, it develops rapidly and is difficult to extinguish, causing immeasurable losses.

With the development of fire dynamics and the continuous progress in simulation technology, performance-based fire prevention design methods have been used in China and abroad to set up safety objectives and quantitative performance criteria according to building use, fire load, and fire scenarios. Analysis tools have been used to evaluate whether fire protection design schemes achieve the preset fire targets. The topic of fire model analysis is currently extensively studied globally. Guillaume et al. [2] performed CFD modeling of the entire facade of Grenfell Tower in the late horizontal stage of the fire spread. Taek-Hum et al. [3] carried out studies according to the fire safety regulations at the time, such as the study of the fire load of wooden constructions and analyses of the performance of fire-heating equipment. Kweon et al. [4], Ekr et al. [5], Chen et al. [6], Menis et al. [7], and others studied the fire load of timberwork buildings, showing that

the fire performance of the wood decreases as the load increases, and a practical load curve–fire resistance design was developed. Wei et al. [8] and Gao et al. [9] used oil pool fire and a Bunsen burner to study the fire performance of typical components of wooden structure buildings. Wang et al. [10], Sun et al. [11], and Yi et al. [12] used the Fire Dynamics Simulator (FDS) to analyze the spread law and the mechanism of wooden frame building fires at different wind speeds. Guo et al. [13], Betting et al. [14], Ding et al. [15], Colin et al. [16], and others reported the temperature changes and the flue gas spread law of buildings under different working conditions using numerical simulations. WG et al. [17] used FDS simulation software to perform multiple sets of experiments on the multi-ignition combined flame phenomenon and compared the various experiments' results, proving the effectiveness of the proposed model.

The correlation between the fire prevention medium and the fire must be fully considered to control and extinguish fires in wooden buildings and to ensure the safety of personnel, property, and the buildings themselves [18]. Halon exhibits good fire-extinguishing performance but generates many bromine and chlorine free radicals, so it is not considered an environmentally friendly green extinguisher [19,20]. Fine-water-mist fire-extinguishing systems exhibit high efficiency, stability, a low cost, sustainability, and environmental friendliness [21]. They are important alternative materials for halogenated alkane fire-extinguishing media and are widely used in many industries. Chiu et al. [22] compared the advantages and disadvantages of fire-extinguishing equipment. The water-mist fire-extinguishing system exhibits a large spray area and can offer a variety of parameter adjustments, making it an optimal fire-extinguishing option. Mahmud et al. [23] carried out experimental and numerical studies on high-pressure water-mist nozzles, and the spray results predicted by the CFD simulation were in good agreement with the experiments. Gupta et al. [24] experimentally studied the factors that influence the effect of fine water mist on the extinguishing of oil pool fires. As the average droplet diameter decreased, the droplet velocity increased, and the fire-extinguishing time gradually shortened. Ye et al. [25] considered the continuous stilted buildings in the Dong area of Guangxi as an example to discuss a fire prevention system, in which the fire prevention intervals of the Dong village buildings and the external-wall spray systems functioned cooperatively. Cheng et al. [26] used Pyrosim software to establish a water-mist screen fire model and to analyze the influence of smoke, temperature, and visibility in a subway tunnel. Li et al. [27] discussed the heat absorption and cooling performance of high-pressure water mist and the effect of droplet size on fire cooling, deriving the fire propagation law of urban underground pipe corridors based on a high-pressure water-mist fire-extinguishing system. Dry water is a new type of fire-extinguishing agent. Lee et al. [28] used the sieving method to separate dry water according to particle size, and by using the wooden bed fire-extinguishing test, they concluded that medium dry water was the best. Ingason et al. [29] used three different side-wall nozzle systems to extinguish wood pallet fires, and they concluded that the pressure parameters of the nozzle determined the efficiency of controlling flame diffusion within the fuel load range. Liu et al. [30] and Ferng et al. [31] discussed the influence of water droplet size on the fire-extinguishing mechanism and determined that it is easier to extinguish fires by using smaller droplets. Yu et al. expounded on the advantages of high-pressure water-mist fire-extinguishing systems in ancient buildings [32]. A study on the water damage loss of wooden components due to spraying showed that the water damage loss of wood is controllable and does not lead to wood corrosion when the water mist acts on the wood components [33].

Material combustion requires combustible substances, combustion aids, and ignition sources. Fine water mist affects all three elements in the fire-extinguishing process. The current research data recognize three mechanisms considered the main principles of water-mist fire extinguishing: heat absorption and cooling through vaporization, isolation of the oxygen asphyxiation fire source, and radiant heat barrier formation [31,34,35]. Ko et al. [36] believe that a full-scale fire test should be conducted to verify whether the fine-water-mist fire-extinguishing standard can be applied to actual fires in wooden structures.

However, it is very difficult to study the fire spread characteristics of stilted wooden buildings using a full-size field-testing method. Most studies are based on simulations, as simulations save costs and are easy to implement, enabling comparisons of the influences of different working conditions on the fire. Thus, this study uses fire simulation software (FDS) to establish a fire model of stilted wooden buildings. The model shape was set with the simulation software, the corresponding conditions were prepared, and the fire-extinguishing effect of stilted buildings with wooden structures in the burning area under the action of fine water mist was studied.

2. Fire Modeling and Setting of Related Parameters

2.1. Stilted Building Model

The typical stilted wooden buildings in Guizhou Province were the research objects in this study. A stilted building usually possesses four rows and three rooms, is built on a slope, and is mostly divided into three floors. The first floor is used as a livestock pen or to pile up debris; the second floor is used for living quarters; and the third floor, the lowest floor, is used to store grains. According to the stilted building model, its size was set to a length \times width \times height of 10 m \times 10 m \times 9 m. A sofa in the living room was set as the fire source of the wooden structure stilted building, and thermocouples (4 in total) were installed every 0.5 m along the central axis of the fire source (−1.7 m, 2.2 m, and 3.5 m) to monitor the room temperature. At the same time, five water-mist nozzles with coordinates of W1 (−2.7 m, −3.8 m, and 6.0 m), W2 (−2.7 m, −3.3 m, and 6.0 m), W3 (−2.7 m, −2.8 m, and 6.0 m), W4 (−2.7 m, −2.3 m, and 6.0 m), and W5 (−2.7 m, −1.8 m, and 6.0 m) were set. A temperature slice with the coordinate $Y = -2.2$ m was set along the center of the fire source to monitor the temperature of the internal section of the room. A thermocouple, A (−1.7 m, −2.7 m, and 5.0 m), was set beside the fire source to monitor the indoor temperature, and a flue gas volume fraction measurement device, B (−3.0 m, −3.0 m, 6.0 m), was set to monitor the volume fraction of the indoor flue gas. The stilted building model and the fire situation are shown in Figure 1.

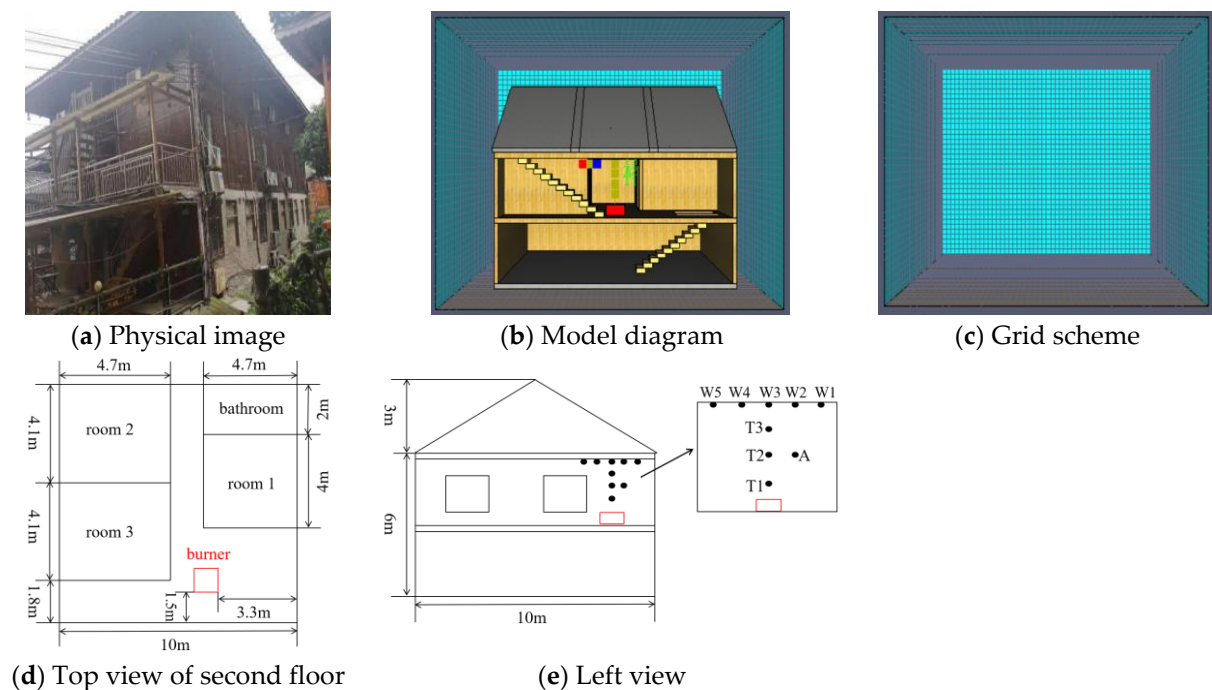


Figure 1. Model of a stilted building.

2.2. Governing Equation

There are two kinds of numerical fire simulation models: field simulations and regional simulations. The field model is based on finite element analyses, and each element follows

the law of the conservation of mass and momentum. The regional model is a model that uses mathematical analyses to determine the evolution of a fire in a confined space. The simulation methods in the FDS usually include a direct numerical simulation (DNS), Reynolds time-equilibrium simulation (RANS), and a large-eddy simulation (LES). In this paper, the large-eddy simulation (LES) is used to describe the turbulent flow of the fire fluid, and it is suitable for large-scale fire simulations. By solving the basic control equations (Equations (1)~(4)), the fire smoke flow and heat transfer processes can be simulated accurately, and the parameters of the fire temperature, velocity, gas concentration, and visibility can be obtained. Its basic mathematical model is as follows [13]:

Mass equation:

$$\frac{\partial \rho}{\partial t} + \nabla \rho \bar{u} = 0 \quad (1)$$

Energy conservation equation:

$$\rho c_p \left(\frac{\partial T}{\partial t} + \bar{u} \cdot \nabla T \right) - \frac{dp_0}{dt} = q + \nabla k \nabla T \quad (2)$$

The equation for the conservation of momentum:

$$\rho \left(\frac{\partial \bar{u}}{\partial t} + \frac{1}{2} \nabla \left| \bar{u} \right|^2 - u \times \omega \right) + \nabla P - \rho g = \nabla \sigma \quad (3)$$

Ideal gas equation of state:

$$P_0(t) = \rho RT \quad (4)$$

where ρ is the flow field density, kg/m³; t is the time; s is the flow field velocity vector, m/s; c_p is the specific heat capacity, J/(kg·K); T is the flue gas layer temperature, K; P_0 is the environmental pressure, Pa; the heat release rate per unit volume, kW/m², is the thermal conductivity coefficient; ω represents the vortices, m/s; P is the flue gas layer pressure, Pa; g is the gravitational acceleration, m/s²; σ is the compressive fluid stress; and R is the general gas constant.

2.3. Parameter Setting and Meshing

(1) Parameter setting: In the numerical simulation in this paper, the ambient temperature was set to 20 °C, and the wind speed was set to 4 m/s because the wooden furniture and its components are the most important combustion materials in the wooden structure stilted building. A T²-fire model was used to express the combustion process [37]. The T²-fire model was calculated using the maximum heat release rate in the fire development, which can be used to describe the process from the slow combustion state to the gradual stabilization of the fire. The model formula is as follows [38]:

$$Q = \alpha T^2 \quad (5)$$

According to the value of the fire growth coefficient α , a T² fire can be divided into four types, namely, a slow fire, a medium-fast fire, a fast fire, and a super-fast fire, and the growth coefficients of the four fire models are shown in Table 1. According to the actual situation of the typical wooden structure buildings in Guizhou Province, combined with the characteristics of wood weathering, a low moisture content, and easy combustion, the fire growth coefficient was between a medium-speed and fast fire, and it was set to 0.01172 kW/s².

Table 1. Fire growth coefficient.

Growth Type	Fire Growth Factor kW/s ²	Typical Combustible Materials
Super-fast	0.18780	Oil pool fire, flammable home decorations, light curtains
Fast	0.04689	Bags stuffed full of stuff, plastic foam
Medium-fast	0.01127	Cotton and polyester items, wooden offices
Slow	0.00293	Heavy wood products

According to Table 2 [39], the maximum heat release rate of the model was set to 2500 kW. According to Equation (5), the fire model achieved stable combustion at 462 s, and the total simulated time was set to 800 s in order to observe the subsequent fire spreading.

Table 2. Maximum heat release rate of typical fire sites.

Typical Fire Sites	Maximum Heat Release Rate/MW
Malls with sprays	5.0
Spray offices and guest rooms	1.5
Public areas with sprays	2.5
Supermarkets and warehouses with sprays	4.0
Spray-free offices and guest rooms	6.0
Public places without spraying	8.0
Spray-free supermarkets and warehouses	20.0

(2) Water-mist parameters: The water-mist parameters critically affect the fire-extinguishing effect. The setting of the fine-water-mist nozzle parameters is shown in Table 3 [18].

Table 3. Water-mist nozzle parameter settings.

Parameter	Setup
Spray speed	5 m/s
Work pressure	10 MPa
Spray angle	60°
Initial nozzle temperature	20.0 °C
Nozzle activation temperature	74.0 °C
Droplets per second	5000

(3) Meshing: The grid division is related to the accuracy of the solution of the control equation, and the finer the mesh, the more accurate the numerical simulation. However, the time required for computer calculations increases exponentially [11]. In the fire plume model of large-eddy simulations, a dimensionless expression $D^* / \delta x$ [40] is used to calculate the flow field accuracy. Many studies have reported that the simulation accuracy and computational efficiency could yield more accurate results when the ignition source feature diameter D^* is 4~16 times higher than the minimum mesh size δx [41–43]. According to Equation (6), the value of D^* is 1.3835, and the range of δx is 0.09–0.35:

$$D^* = \left(\frac{Q}{\rho_{\infty} C_p T_{\infty} \sqrt{g}} \right)^{\frac{2}{5}} \quad (6)$$

In Equation (6), D^* is the characteristic diameter of the ignition source, m; Q is the total heat release rate of the ignition source, kW; ρ is the air density, kg/m³; C_p is the specific heat capacity at a constant pressure, J/(kg·K); T is the ambient temperature, K; and g is the gravitational acceleration, m/s². This paper divides the grid into $0.30 \times 0.30 \times 0.30$ based on the computer running state and the simulation time, and the model is divided into 81,400 grids, as shown in Figure 1c.

3. Simulation Results and Analysis

3.1. Influence of Droplet Size on the Fire-Extinguishing Effect

To compare the fire-extinguishing effects of the water mist with different droplet sizes, a free combustion system without fine water mist was simulated, and the effects of the different droplet sizes were numerically simulated when the water-mist flow rate was 8 L/min, and the nozzle density was 5. The starting condition of the fine-water-mist nozzle was when the temperature measured by the temperature detector reached 74 °C; that is, after 148 s of the simulated combustion, the fine-water spray was applied in the room. The temperature change curves for the different droplet sizes under different working conditions were measured using thermocouple A, as shown in Figure 2. When the droplet size is 150 μm or less, the cooling effect of the fine-water-mist fire-extinguishing system is better. The fire-extinguishing effect of the water mist with a larger particle size is relatively poor. When the water mist of each particle size is used for the fire-extinguishing simulation, the temperature increases continuously with the advancement of time. When the temperature rises to a certain temperature, the temperatures of the 100, 150, and 200 μm particle size measuring points begin to decrease, followed by a decrease in the particle size measuring points of 300 μm and free burning. The temperature of the measuring point then shows a certain trend. With a decrease in the droplet size, the speed of the temperature drop is accelerated. The reason for this is that the fine-water-mist particle size of 150 μm or less is small; the volume is rapidly expanded after heating; the evaporation rate is faster; the oxygen is squeezed out and isolated around the flame, reducing the oxygen concentration required for combustion; and the suppression of the flame is accelerated, thus achieving a rapid fire-extinguishing effect. However, the contact area between the water mist with a large droplet size and the flue gas is small, which attenuates the evaporation effect of the water mist to a certain extent and greatly weakens the cooling effect.

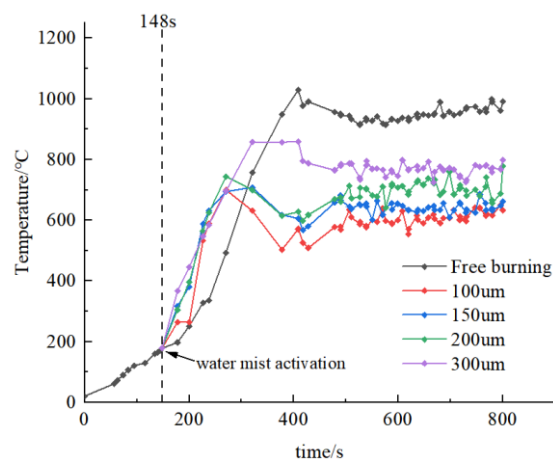


Figure 2. Temperature values measured by thermocouple A at different droplet sizes.

The temperature profile of the center of the flame (480 s) after the fire field begins to burn steadily at different droplet sizes is shown in Figure 3. The temperature values extracted at 200, 400, 600, and 800 s are shown in Table 4.

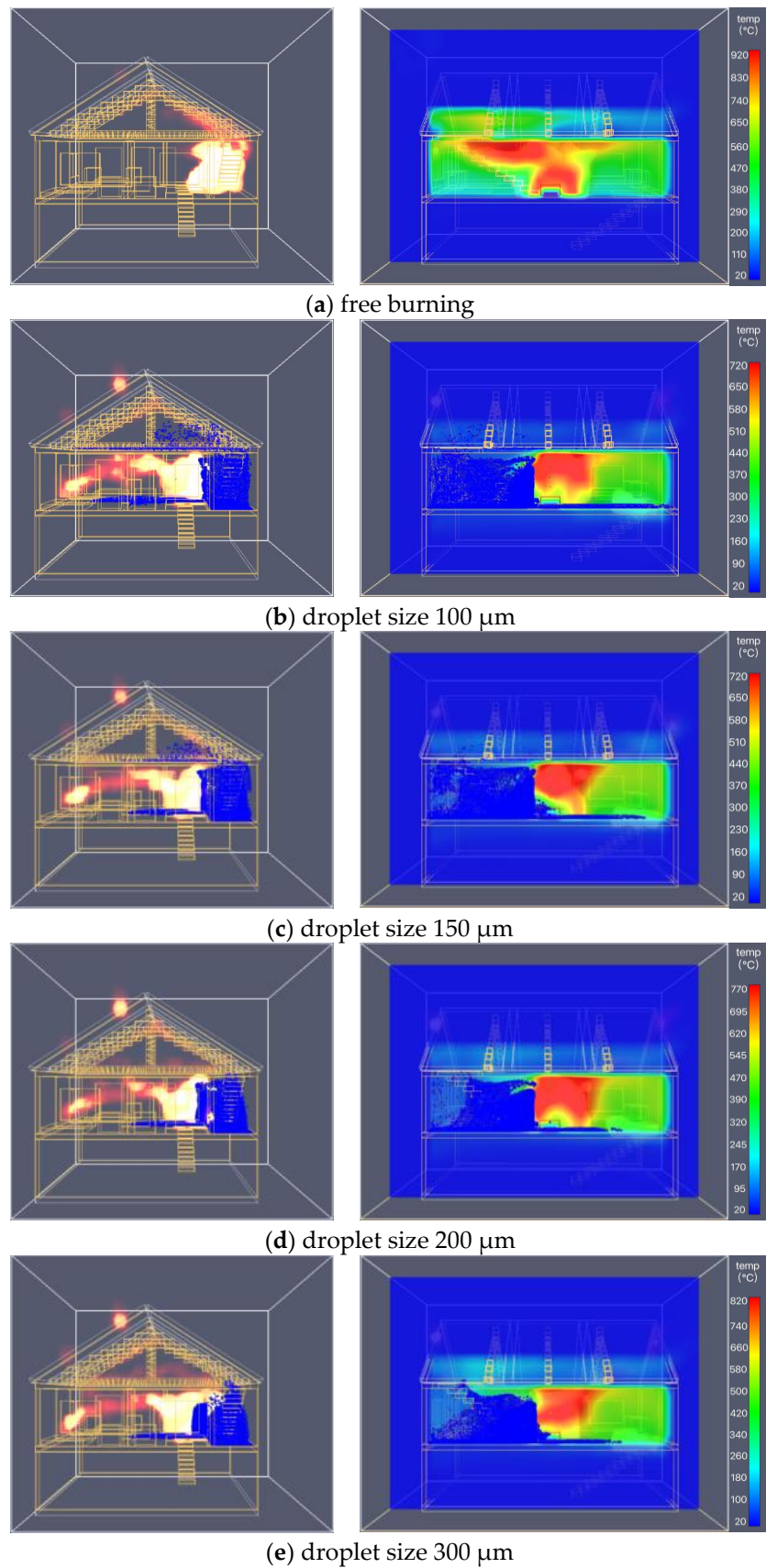


Figure 3. Temperature profiles of different droplet sizes at 480 s.

Table 4. Temperatures at 200, 400, 600, and 800 s at different droplet sizes.

Working Conditions	Water-Mist Flow (L/min)	Number of Water-Mist Sprinklers	Water-Mist Droplet Size (μm)	200 s	400 s	600 s	800 s
free burning	0	0	0	251	989	929	992
	8	5	100	395	501	592	634
different droplet sizes	8	5	150	381	580	657	662
	8	5	200	264	670	724	777
	8	5	300	446	795	770	799

Figure 3 and Table 4 show that the temperature in the presence of the fine water mist is lower than the temperature of free combustion, while the fire is relatively small. The droplet size affects the temperature change, and the temperature of the fire field and the rate of fire potential significantly decline as the droplet size decreases. In Table 4, at 200, 400, 600, and 800 s, the differences between the highest and lowest temperatures are 195, 488, 337, and 358 °C, respectively. When the mist droplet sizes are 100, 150, 200, and 300 μm , the temperature measurement point at 200 s is higher than the temperature measurement point of the free combustion without the water mist. This is due to the temperature fluctuation caused by the opening of the water-mist fire-extinguishing system. At about 400 s, the temperature of each particle size tends to be balanced, and then the temperature fluctuation is small. The water mist with a droplet size of 100 and the water mist with a droplet size of 150 μm have similar temperatures. It can be seen from the fire and the highest point temperature in Figure 3 that the water mist with a droplet size of 150 μm or below has a good fire-extinguishing effect. The larger the relative surface area, the longer the residence time of the droplets in the hot flue gas, and the longer the evaporation heat absorption time, the greater the heat absorption by evaporation. It can be seen that the fire-extinguishing performance of the small droplet size is better than that of the large droplet size. This is consistent with the current research [30,31].

3.2. Influence of Different Spray Flow Rates on the Fire-Extinguishing Effect

Figure 4 shows the temperature change curves measured by thermocouple A at different fine-water-mist spray flows. The fine-water-mist fire-extinguishing system activates after the fire occurs at 148 s. In the combustion area, the opening of the fine-water-mist fire-extinguishing system has a significant cooling effect. The temperature continues to rise rapidly when the water-mist fire-extinguishing system is not activated, and the measured temperature reaches a peak of 1029 °C at 409 s. After applying the fine water mist to the room at 148 s, the room flue gas temperature decreases significantly. When the flow rate is 2.4 L/min, the fine water mist quickly reduces the temperature to 938 and 787 °C. When the flow rate is 6 L/min, the room temperature rises within 150 s, and the temperature stabilizes at about 800 °C after reaching stable combustion. When the fine-water-mist flow rate is 8 L/min, the flue gas temperature quickly drops to 571 °C, and the fire temperature stabilizes at about 600 °C after 30 s. A comprehensive comparison found that 8 L/min exhibits the highest cooling efficiency and better effects because the fine water mist is atomized and mixed with the high-temperature flue gas, which reduces the temperature difference between the flue gas and the lower cold air and subsequently slows down the flue gas flow speed. With the decrease in the particle size of the water mist and the increase in the flow rate, the air quality velocity decreases gradually, absorbing a large amount of heat. At the same time, the fine water mist can also effectively reduce thermal convection, block the thermal radiation in the fire area, and reduce the temperature of the fire field.

The profiles of the flame center temperatures (480 s) when the fire field reaches stable combustion at different spray flow rates are shown in Figure 5. The temperature values at 200, 400, 600, and 800 s are shown in Table 5.

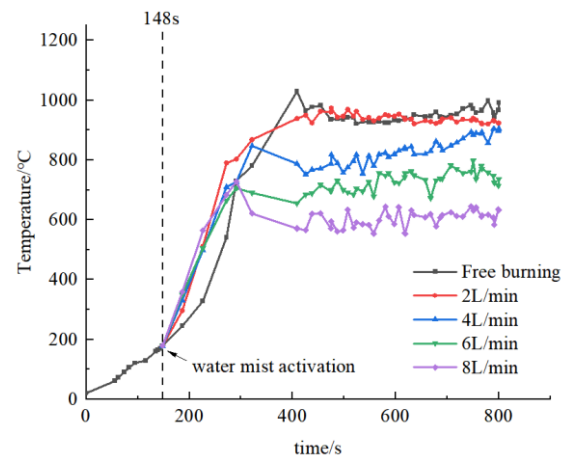


Figure 4. Temperatures measured by thermocouple A at different spray flow rates.

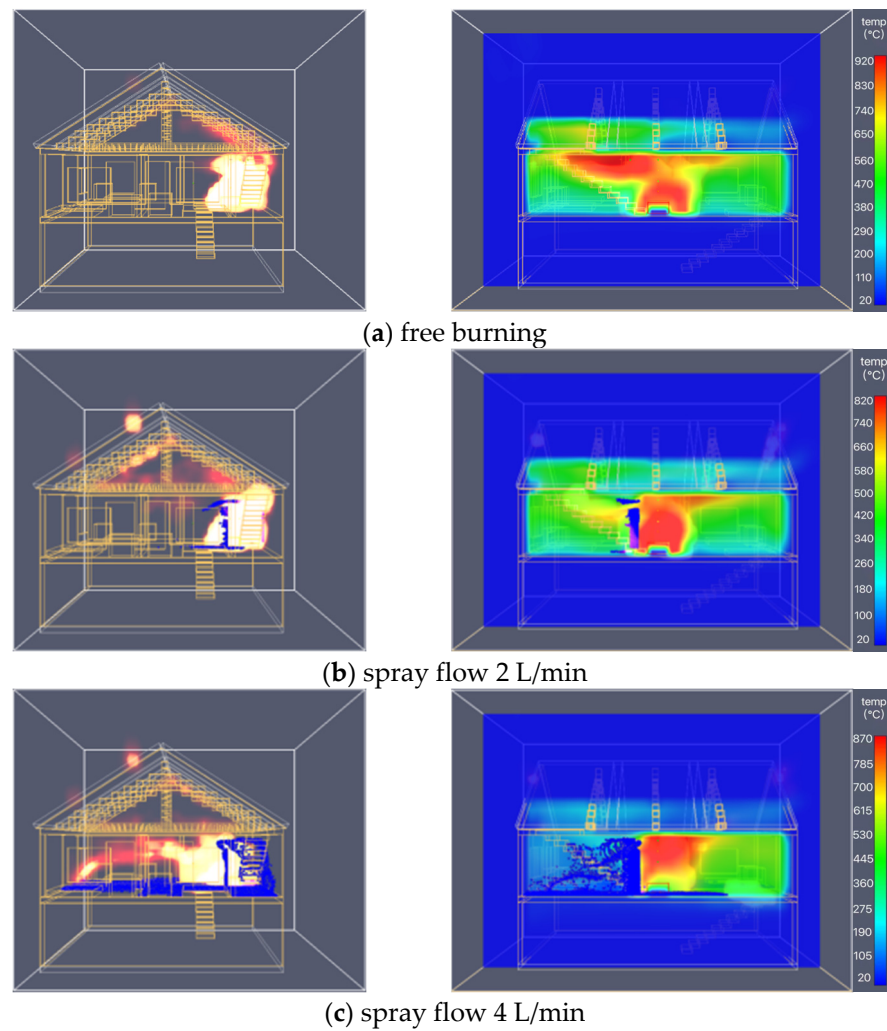


Figure 5. Cont.

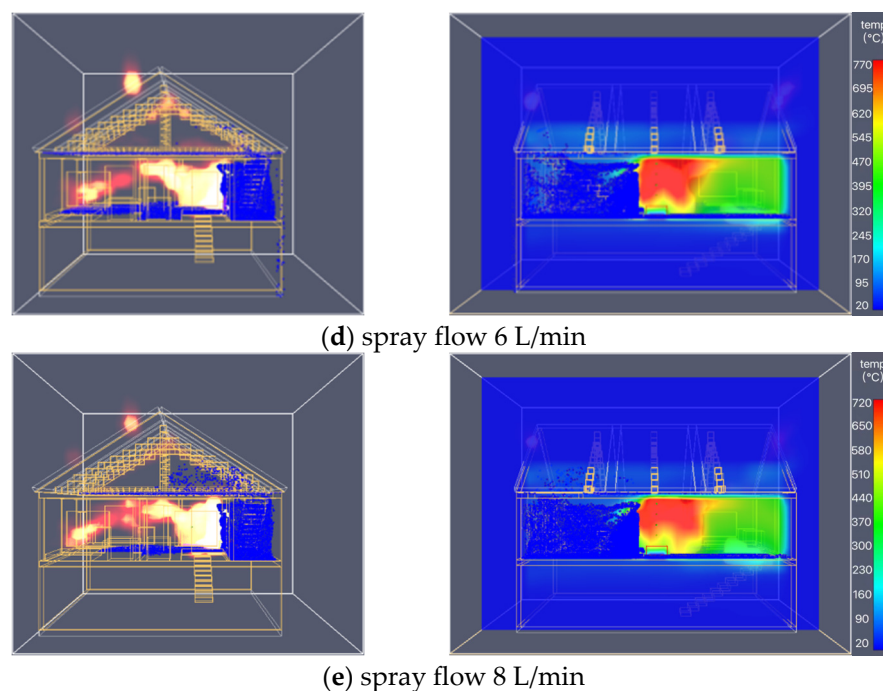


Figure 5. Temperature profiles of different spray flows at 480 s.

Table 5. Temperatures at 200, 400, 600, and 800 s at different water-mist flows.

Working Conditions	Water-Mist Flow (L/min)	Number of Water-Mist Sprinklers	Water-Mist Droplet Size (μm)	200 s	400 s	600 s	800 s
free burning	0	0	0	251	989	943	992
different spray flows	2	5	100	377	933	929	924
	4	5	100	409	759	824	905
	6	5	100	407	572	702	736
	8	5	100	395	501	592	634

Figure 5 and Table 5 show that, when the spray flow rate is 8 L/min, the fire potential is smaller than that in the other cases, and the temperature in the entire combustion space is relatively low. At 200, 400, 600, and 800 s, the differences between the highest and lowest temperatures are 158, 488, 351, and 358 °C, respectively. The spray flow rate of the fine water mist affects the fire site temperature. When the spray flow rates are 2, 4, 6, and 8 L/min, the temperature measuring points are higher than the free combustion temperature measuring point at 200 s. Similarly, the temperature of each measuring point shows a certain trend after 400 s, and the fire field temperature increases with the flow rate, decreasing the fire potential. Under adequate working conditions, the maximum spray flow rate should be selected within the specified range to achieve the best fire-extinguishing effect.

3.3. Influence of Different Nozzle Densities on Fire-Extinguishing Effect

We set the nozzle density in this paper to 1, 3, and 5 with a fine water droplet diameter of 100 μm and a water droplet flow rate of 8 L/min to analyze the influence of water nozzle density on fire extinguishing at the fire site. The temperature data collected by the thermocouple 0.5 m above the fire source were compared, and the results are shown in Figure 6. After 400 s, the temperature of the fire field increases with the nozzle density, and the fire-extinguishing effect gradually increases. This occurs because, when the fire spreads toward the fine-water-mist fire-extinguishing area, its spreading speed is affected by the water mist, and it begins to slow down. When a water-mist nozzle is set, there is little difference between the temperature of the water-mist-cooling fire field and the free

combustion temperature. This is because the water-mist area formed by a single water-mist nozzle is small, and the fire-extinguishing effect on the fire site is not obvious. When the density of the nozzles is increased, the water mist between the nozzles overlaps, and the overlapping water-mist porosity is relatively small, which can prevent the spread of the fire.

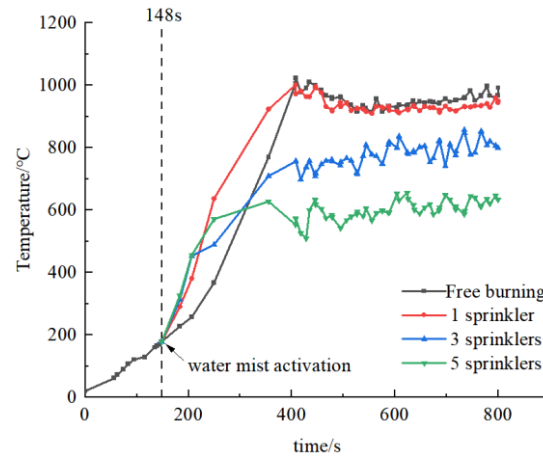


Figure 6. Temperatures measured by thermocouple A at different nozzle densities.

The flame center temperature profiles (480 s) after the fire field begins to burn steadily under different nozzle density conditions is shown in Figure 7. The temperature values at 200, 400, 600, and 800 are extracted, as shown in Table 6.

Table 6. Temperatures of different nozzle densities at 200, 400, 600s, and 800.

Working Conditions	Water-Mist Flow (L/min)	Number of Water-Mist Sprinklers	Water-Mist Droplet Size (μm)	200 s	400 s	600 s	800 s
free burning	0	0	0	251	989	929	992
different numbers of nozzles	8	1	100	385	961	914	950
	8	3	100	407	654	770	799
	8	5	100	395	501	592	634

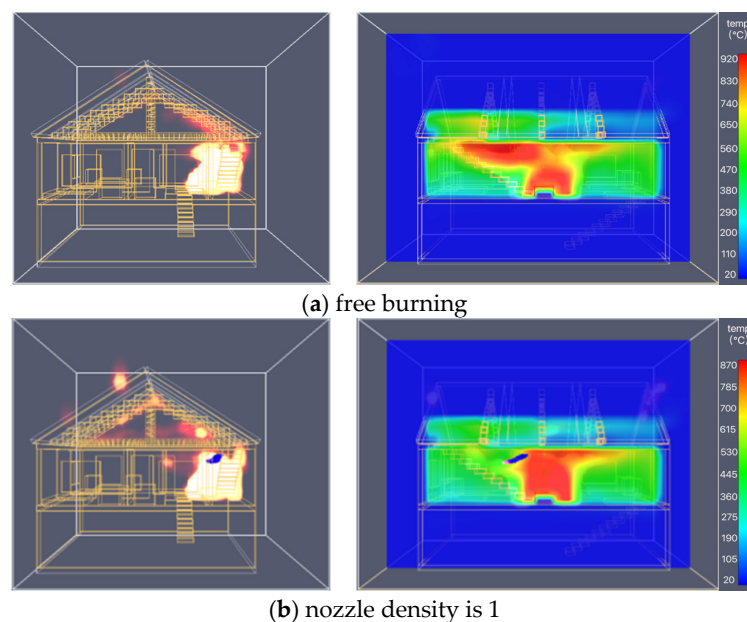


Figure 7. Cont.

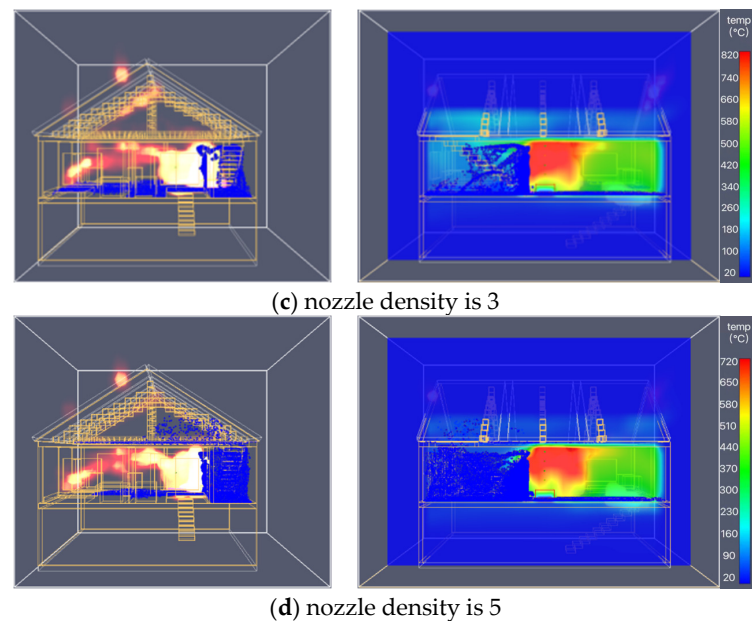


Figure 7. Temperature profiles of different nozzle densities at 480 s.

Figure 7 and Table 6 show that, after adding the fine water mist at 200 s, the working conditions are lower than the temperature of free combustion, and the fire potential is relatively small. The density of the nozzle affects the change in the fire field temperature. The faster the increase in the density of the fine-water-droplet nozzle, the faster the decrease in the temperature of the fire field. At 200, 400, 600, and 800 s, the differences between the highest and lowest temperatures are 156, 488, 337, and 358 °C, respectively. In Table 6, it can be seen that, when the nozzle density is 1, the temperature is not much different from the free combustion temperature. A nozzle density of 3 can better suppress the fire temperature. When the nozzle density is 5, the temperature change curve decreases from 400 s to about 500 °C, and then the temperature increases and stabilizes at about 600 °C.

4. Conclusions

By carrying out an FDS simulation, this paper studies the fire-extinguishing properties of fine-water-mist fire-extinguishing systems under different fine-water-mist droplet sizes, fine-water-mist flow rates, and nozzle densities. The analysis results are as follows:

- (1) The fine-water-mist fire-extinguishing system exhibits heat-absorbing and cooling effects on fires in stilted buildings with wooden structures, and they can inhibit the further development of fires and play a positive role in fire emergency rescue.
- (2) When the flow rate of the fine water mist and the density of the nozzle remain unchanged, the fine water mist with a small droplet diameter exhibits a good evaporative heat absorption effect. The smaller the particle size, the faster the vaporization rate and the better the cooling effect. The cooling effect of droplets with a size of 150 μm or less is better than that of droplets with sizes of 200 μm and 300 μm .
- (3) When the particle size and nozzle density of the fine water fog remain unchanged, the temperature of the fire field decreases faster with the flow rate, and the cooling efficiency is the highest when the flow rate is 8 L/min. If conditions permit, the maximum spray flow can be selected within the specified range to achieve the best fire-extinguishing effect.
- (4) When the droplet size and the flow rate of the fine water mist remain unchanged, the fire-extinguishing effect at the fire site is not obvious when setting up a water-mist nozzle. When the density of the water nozzles is increased, the water mist between the nozzles overlaps, making the porosity of the water mist smaller and preventing the spread of the fire.

The above research mainly considers the influences of different water-mist characteristics and nozzle arrangements on fire temperature. The research results have certain reference significance for application in fire scenarios in various fields. In addition, the influence of external environmental conditions, such as wind speed, on the application of water mist is not examined in this paper, but it will be examined in subsequent research.

Author Contributions: Conceptualization, X.Z.; software, X.Z. and Y.C.; formal analysis, X.Z.; investigation, N.W.; data curation, X.Z.; writing—original draft preparation, X.Z.; writing—review and editing, S.W.; supervision, S.W.; project administration, S.W. All authors have read and agreed to the published version of the manuscript.

Funding: This work was funded by the Talent Introduction Research Fund of Guizhou University (Guizhou University Talent Fund Cooperation Project (2016) No. 58) and the Guizhou Province Science and Technology Support Project (Qiankehe Support (2019) 2889).

Data Availability Statement: The model and relevant data involved in the research process have appeared in the paper.

Conflicts of Interest: The authors declare no conflict of interest.

References

1. Ministry of Emergency Management. Ministry of Emergency Management of the People's Republic of China. Regular Press Conference in January 2022 [EB/OL]. 2022. Available online: <https://www.mem.gov.cn/xw/xwfbh/2022n1y20rxwfbh/> (accessed on 20 January 2022).
2. Guillaume, E.; Dréan, V.; Girardin, B.; Fateh, T. Reconstruction of the grenfell tower fire—part 4: Contribution to the understanding of fire propagation and behaviour during horizontal fire spread. *Fire Mater.* **2020**, *44*, 1072–1098. [CrossRef]
3. Oh, T.H.; Park, C.S. Improvement of Performance based wooden building National Fire Safety Codes. *J. Korea Saf. Manag. Sci.* **2016**, *18*, 83–92.
4. Oh-Sang, K. The Study on Compartment Fire Experiment According to Fire Load. *Fire Sci. Eng.* **2017**, *31*, 16–22.
5. Ekr, J.; Caldova, E.; Vymlatil, P.; Wald, F.; Kuklikova, A. Timber steel-fibre-reinforced concrete floor slabs subjected to fire. *Eur. J. Wood Prod.* **2018**, *76*, 201–212. [CrossRef]
6. Chen, L.Z.; Xu, Q.F.; Leng, Y.B.; Harries, K.A.; Wang, Z.L. Experimental study of performance of engineered bamboo beams exposed to three-sided standard fire. *Fire Saf. J.* **2019**, *106*, 52–60. [CrossRef]
7. Menis, A.; Fragiacomio, M.; Clemente, I. Fire resistance of unprotected cross-laminated timber floor panels: Parametric study and simplified design. *Fire Saf. J.* **2019**, *107*, 104–113. [CrossRef]
8. Wei, S.; Yang, H.; Gao, B.; Cheng, H.; Lu, R.; Dong, L. Experimental research on temperature distribution and charring rate of typical components of wood structure building. *J. Fire Sci.* **2022**, *40*, 134–152. [CrossRef]
9. Gao, B.; Wei, S.; Du, W.; Yang, H.; Chu, Y. Experimental Study on the Fire Resistance Performance of Partition Board under the Condition of Small Fire Source. *Processes* **2021**, *9*, 1818. [CrossRef]
10. Wang, Y.N.; Qiu, H. Numerical analysis of spreading law of ancient timber building group fire based on FDS. *China Saf. Sci. J.* **2014**, *24*, 26–32.
11. SUN, G.L. Analysis of ancient buildings fire spreading based on PyroSim. *Fire Sci. Technol.* **2016**, *35*, 214–218.
12. Yi, X.L.; Zheng, L.P. Performance-based fire protection assessment ancestral temple in canton based on fire dynamics simulator. *Build. Sci.* **2021**, *37*, 89–97+103.
13. GUO, F.L.; Chen, P.; Wang, X.Y.; Jin, K. On Characteristics of Fire spreading Among Stilt-styled House Complex with Timber Structure. *Cite Towns Constr. Guangxi* **2012**, *10*, 85–90.
14. Betting, B.; Varea, E.; Gobin, C.; Godard, G.; Lecordier, B.; Patte-Rouland, B. Experimental and numerical studies of smoke dynamics in a compartment fire. *Fire Saf. J.* **2019**, *108*, 102855. [CrossRef]
15. Ding, H.C.; Xu, Y.D.; Deng, Q.L.; Lian, Z. Simulation study on influence of fire smoke flow on evacuation in high-rise buildings. *China Saf. Sci. J.* **2020**, *30*, 118–124.
16. Colin, C.; Jason, J.; Jason, P. Sensitivity of atypical lateral fire spread to wind and slope. *Geophys. Res. Lett.* **2016**, *43*, 1744–1751.
17. Weng, W.G.; Kamikawa, D.; Fulcoda, Y. Study on flame height of merged flame from multiple fire sources. *Combust. Sci. Technol.* **2004**, *76*, 2105–2123. [CrossRef]
18. Wu, S.F.; Yuan, Y.P. Simulation Research on Suppression and Extinguishment of Fires in a Ship Engine Room by Water Mist based on FDS. *Shipbuild. China* **2020**, *61*, 170–187.
19. Wang, Z.H. Application of high-pressure water mist fire extinguishing system in Shanghai Tower. *Water Wastewater* **2015**, *05*, 80–81.
20. Xiong, W.R. Discussion on the application of water mist fire extinguishing system in cultural relics and ancient buildings. *China New Commun.* **2017**, *19*, 90–91.

21. Xu, W. Study on the Mechanism of Inhibition of Hydrocarbon Flame by Some Halon Substitutes. Ph.D. Thesis, University of Science and Technology of China, Hefei, China, 2017.
22. Chiu, C.W.; Li, Y.H. Full-scale experimental and numerical analysis of water mist system for sheltered fire sources in wind generator compartment. *Process Saf. Environ. Prot.* **2015**, *98*, 40–49. [[CrossRef](#)]
23. Mahmud, H.M.I.; Moinuddin, K.A.M.; Thorpe, G.R. Experimental and numerical study of high-pressure water-mist nozzle sprays. *Fire Saf. J.* **2016**, *81*, 109–117. [[CrossRef](#)]
24. Gupta, M.; Pasi, A.; Ray, A.; Kale, S.R. An experimental study of the effects of water mist characteristics on pool fire suppression. *Exp. Therm. Fluid Sci.* **2013**, *44*, 768–778. [[CrossRef](#)]
25. Ye, Y.B.; Zhai, Y.Y.; Ma, L.J.; Zhang, Y.P.; Ke, H.Y. Numerical simulation method for controlling fire spread in stilted building of Dong nationality. *Fire Sci. Technol.* **2019**, *38*, 814–817.
26. Cheng, M.; Li, Y.; Ren, Y.X. Analysis on the effect of fine water mist curtain blocking fire smoke spreading in subway tunnel. *Fire Sci. Technol.* **2019**, *38*, 519–521.
27. Li, T.; Su, Z.M.; Chen, L.F.; Hu, A.-L.; Zhang, J. Cooling efficiency of high pressure water mist on fire urban underground pipe gallery. *Fire Sci. Technol.* **2019**, *38*, 966–969.
28. Lee, E.; Choi, Y. Effects of particle size of dry water on fire extinguishing performance. *J. Korean Soc. Saf.* **2019**, *34*, 28–35.
29. Ingason, H.; Li, Y.Z. Large scale tunnel fire tests with different types of large droplet fixed fire fighting systems. *Fire Saf. J.* **2019**, *107*, 29–43. [[CrossRef](#)]
30. Liu, H.; Wang, C.; Cordeiro, I.M.D.C.; Yuen, A.C.Y.; Chen, Q.; Chan, Q.N.; Kook, S.; Yeoh, G.H. Critical assessment on operating water droplet sizes for fire sprinkler and water mist systems. *J. Build. Eng.* **2020**, *28*, 100999. [[CrossRef](#)]
31. Ferng, Y.M.; Liu, C.H. Numerically investigating fire suppression mechanisms for the water mist with various droplet sizes through FDS code. *Nucl. Eng. Des.* **2011**, *241*, 3142–3148. [[CrossRef](#)]
32. Yu, P.W.; Yang, W.Q.; Wu, J.K.; Zhang, F. Discussion on the application of high pressure water mist fire extinguishing system in the fire protection design of ancient buildings. *Water Wastewater Eng.* **2021**, *47*, 89–92+101.
33. Yu, P.W.; Wang, Y.X.; Guo, Q.B.; Yang, W.; Qiao, Y.; Shi, X. Research on water damage of ancient wooden structure after spraying with high pressure water mist fire extinguishing system. *Fire Sci. Technol.* **2021**, *40*, 668–671+691.
34. Li, Z.N.; Su, H.; Xiang, T.Y. Study on effect of ignition sources on flashover of ancient timber structure. *Fire Sci. Technol.* **2017**, *36*, 594–599.
35. McGrattan, K.B.; Baum, H.R.; Rehm, R.G.; Hamins, A.; Forney, G.P.; Floyd, J.E.; Hostikka, S.; Prasad, K. *Fire Dynamics Simulator—Technical Reference Guide*; National Institute of Standards and Technology, Building and Fire Research Laboratory: Gaithersburg, MD, USA, 2000.
36. Ko, Y.; Kinateder, M.; Elsagan, N. Water Mist Systems in Protection of Mass Timber Buildings. In *International Scientific Conference on Woods & Fire Safety*; Springer: Cham, Switzerland, 2020; pp. 404–409.
37. Yuan, C.Y.; Fang, G.Z.; Zheng, G.K.; Li, Y. Temperature field analysis of ancient timber frame structure in the fire. *Fire Sci. Technol.* **2019**, *38*, 345–348.
38. Lin, C.S.; Wang, S.C.; Hung, C.B.; Hsu, J.H. Ventilation effect on fire smoke transport in a townhouse building. *Heat Transf.—Asian Res. Co-Spons. Soc. Chem. Eng. Jpn. Heat Transf. Div. ASME* **2006**, *35*, 387–401. [[CrossRef](#)]
39. Yuan, C.Y.; Zheng, G.K.; Lan, Y.J.; Wang, P.F. Study on fire characteristics of ancient buildings with brick-wood structure under different fire scenes. *J. Saf. Sci. Technol.* **2019**, *15*, 158–164.
40. Jones, W.W.; Peacock, R.D.; Forney, G.P.; Reneke, P.A. *CEAST—Consolidated Model of Fire Growth and Smoke Transport (Version 6)*; NIST Special Publication: Gaithersburg, MD, USA, 2005; p. 1026.
41. Harmathy, T.Z.; Mehaffey, J.R. *Design of Buildings for Prescribed Levels of Structural Fire Safety*; ASTM International: West Conshohocken, PA, USA, 1985.
42. Downie, B.; Polymeropoulos, C.; Gogos, G. Interaction of a water mist with a buoyant methane diffusion flame. *Fire Saf. J.* **1995**, *24*, 359–381. [[CrossRef](#)]
43. McCaffrey, B.J. Jet diffusion flame suppression using water sprays—An interim report. *Combust. Sci. Technol.* **1984**, *40*, 107–136. [[CrossRef](#)]

Disclaimer/Publisher’s Note: The statements, opinions and data contained in all publications are solely those of the individual author(s) and contributor(s) and not of MDPI and/or the editor(s). MDPI and/or the editor(s) disclaim responsibility for any injury to people or property resulting from any ideas, methods, instructions or products referred to in the content.